Ballistic transport and tunnelling magnetoresistance in tunnel junctions

2002 J. Phys.: Condens. Matter 14 4365

(http://iopscience.iop.org/0953-8984/14/17/309)

INSTITUTE OF PHYSICS PUBLISHING JOURNAL OF PHYSICS: CONDENSED MATTER

J. Phys.: Condens. Matter **14** (2002) 4365–4378 PII: S0953-8984(02)26469-3

Ballistic transport and tunnelling magnetoresistance in tunnel junctions

A H Davis and J M MacLaren

Department of Physics, Tulane University, New Orleans, LA 70118, USA

E-mail: davis@anvil.nrl.navy.mil

Received 3 July 2001, in final form 11 March 2002
Published 18 April 2002
Online at stacks.iop.org/JPhysCM/14/4365

Abstract

In this paper we report the results of a theoretical study of the ballistic tunnelling of electrons in magnetic tunnel junctions. We show how first-principles band-structure calculations and published magnetization data can be used as inputs to the model, which is then used to predict the magnetoresistance of a tunnel junction. This approach provides a convenient way to examine effects not readily treated by purely first-principles calculations such as finite bias and finite temperature as well as providing a way to treat the amorphous nature of most tunnelling barriers. Ultimately, the model is used to show how the tunnelling magnetoresistance depends on extrinsic factors such as applied bias, and temperature, as well as on the intrinsic properties of the junction such as the barrier height and thickness. The model generates the asymmetry in the magnetoresistance often seen for forward and reverse bias in asymmetric junctions.

1. Introduction

A magnetic tunnel junction (MTJ) is a device in which a thin insulator is sandwiched between two ferromagnetic layers, one of whose magnetization (M) can be independently switched. MTJs have two stable states: a low-resistance one in which the magnetizations in the ferromagnetic layers are parallel, and a high-resistance one where the magnetizations are antiparallel. The large percentage change in resistance for small applied fields renders them useful as ultrasensitive field detectors and their two-state capability makes them attractive for use in magnetoelectronic devices. The tunnelling magnetoresistance ratio (TMR $= \Delta R/R$) for this system is defined as the difference between the antiparallel and parallel resistance divided by the antiparallel resistance. In this paper we use the *optimistic* definition of the TMR found by dividing by the smaller parallel resistance:

$$\mathrm{TMR} = \frac{R_X - R_\parallel}{R_\parallel} \tag{1}$$

where the symbol X is used to indicate antiparallel alignment of the M in the two leads.

0953-8984/02/174365+14$30.00

Julliere formulated the first and simplest expression for the TMR [18], in which the tunnelling matrix elements associated with the barrier are assumed to be spin independent. The Julliere model roughly predicts the trends in tunnelling with changing P, though often junctions with chemically similar electrodes can have very different values of the TMR [52] as a result of the barrier itself, a factor neglected in this model. The *optimistic* form of Julliere's equation is

$$\mathrm{TMR} = \frac{2P_L P_R}{(1 - P_L P_R)}, \tag{2}$$

where P for a particular electrode is defined by

$$P = \frac{N_\uparrow - N_\downarrow}{N_\uparrow + N_\downarrow}, \tag{3}$$

where $N_\uparrow$ ($N_\downarrow$) is the fraction of up (down) states which *participate* in the tunnelling.

In general, the TMR depends on the relative alignment of M in the electrodes [18,34,42], falls with increasing temperature (T) and applied bias (V_{bias}) [34, 35], falls with increasing thickness (d) [46], but can be quenched for very thin barriers [32, 36]. The TMR rises with increasing barrier height (V_{bar}), P, or M [34,36]. Annealing can improve the TMR, presumably because it results in higher or thinner barriers [43, 46]. The temperature dependence of the TMR ($\Delta\mathrm{TMR}(T)$) is more severe than the temperature dependence of either M ($\Delta M(T)$) or P ($\Delta P(T)$) in the individual electrodes [17, 35], and normal metal in the interface regions suppresses the TMR [36]. Smaller starting values of the TMR lead to a greater temperature and bias dependence [33] with the least severe bias dependence seen for high, thin barriers [34,46]. Dissimilar electrodes produce asymmetry in the current voltage (I–V) characteristics and $\mathrm{TMR}(V_{\mathrm{bias}})$ for positive and negative V_{bias} [33, 36]. Asymmetry has also been seen for similar electrodes [5, 23].

There have been numerous attempts to model spin-dependent tunnelling in magnetic tunnel junctions, including first-principles work [7, 8, 50]. First-principles treatments of the problem face two significant complications. First, the difficulty in treating the barrier, which is typically amorphous Al_2O_3, and second, the problem of finite bias and temperature, which means dealing with non-equilibrium states. Other theoretical treatments of the tunnelling problem also rely on simple models that are usually able to reproduce some but not all of the experimental observations. These include the Julliere model [18] and generalizations to finite temperature [39], wherein a temperature-dependent polarization was used. However, in order to fit the measured conductance, a parametrized spin-independent contribution was included. A tight-binding calculation by Mathon [29] examined trends that resulted from varying barrier parameters. No actual comparisons to experimental data were made, though the trends found in our model as the barrier thickness and height were adjusted were also found in this work. Various models based upon free-electron tunnelling [9,28,42,54] have been studied. Slonczewski [42] considered the limit of a thick barrier and found a similar expression to that derived by Julliere; however, the predictions of this model tend to underestimate measured TMR values. This underestimate is a result of taking the asymptotic limit. In calculations other than our own, no direct comparisons to measured data were made; rather trends were examined and predictions made for resonant tunnelling in double-barrier systems. Other approaches based on model Hamiltonian calculations [15, 53] can also reproduce measured TMR values and the dependence on bias voltage or temperature. However, these approaches require the use of adjustable parameters. Finally, models have been proposed that rely on the introduction of extrinsic transport mechanisms and additional parameters [17, 52] in order to reproduce experimental TMR data. In all of these different models the basic quantum mechanical model of tunnelling is used, though they differ in the detail of their treatment of

both applied bias and temperature, and the level of detail used in the description of the lead states and the barrier. Agreement with experiment often requires the use of some adjustable parameters.

The model presented in this article is a free-electron approach which uses first-principles calculations as an input, making it possible to treat amorphous barriers phenomenologically, and the non-equilibrium cases of finite bias and temperature. Unlike most other free-electron models, the approach is able to quantitatively reproduce most of the experimentally observed trends with only a single parameter: the barrier height, if the barrier thickness is known. If this thickness is not known then this can be adjusted to ensure an accurate fit to the parallel and antiparallel conductances.

The principal assumption that makes this model both accurate and computationally efficient is that only a subset of the density of states (DOS) in the leads, the free-electron-like states, are responsible for the tunnelling behaviour. These bands are then parametrized with parabolic fits to the results of first-principles density functional calculations. Application of a bias voltage is assumed to lower the chemical potential of the downstream ferromagnetic lead and produce a linear variation in potential in the barrier region. A second assumption is that these tunnelling states are resident in exchange-split bands and that the splitting of the bands is directly proportional to the temperature-dependent magnetization (average magnetic moment per volume, $M(T)$) of the leads, as in a Stoner picture. This permits a phenomenological model of the temperature dependence of the TMR—by allowing the exchange splitting of the tunnelling bands to decrease with temperature in a manner consistent with the temperature variation of the magnetization. In transition metals, the itinerant free-electron-like bands that are responsible for the tunnelling current are seen experimentally via photoemission to follow a Stoner-like behaviour in contrast to the other d bands that dominate the moment.

2. Exchange splitting and magnetization

Table 1 summarizes some of the magnetic data for the 3d transition metals. There is a correlation between the magnetic moments (m) and the exchange splitting (ΔE_{ex}) in the 3d ferromagnets, as would be anticipated from a simple model of exchange-split d bands. We see that within an error of a few per cent,

$$\Delta E_{\mathrm{ex}} \approx mJ \approx \alpha M, \tag{4}$$

where the J are the exchange integrals as calculated by Brooks [6], M is the magnetization, and the constant α is the product of the exchange integral and the cell volume. Shimizu *et al* [40] provided a more rigorous derivation of the same relationship for the exchange splitting in Fe and Ni. They associated α with the molecular-field coefficient and found it to be only mildly dependent on temperature—nearly a constant below room temperature. For instance, the change in α for Fe is only about 2.5% between 0 and 300 K.

The experimental angle-resolved photoemission shows that the exchange splitting of the dispersive d bands in Fe and Ni varies with temperature [1,13,19,20] and that ΔE_{ex} was directly proportional to the bulk $M(T)$. In contrast, for the less dispersive, more localized d bands much smaller changes were observed, consistent with the viewpoint of localized moments present at and above the Curie temperature. MacDonald *et al* [27] noted that the temperature-dependent shift of the spin spectral weight in itinerant electron ferromagnets is proportional to the suppression of the magnetic moment.

Takahashi and Mitsui [47] studied the split conduction bands in magnetic semiconductors where ΔE_{ex} and M were considered to be proportional to the thermal average over fluctuating spin states ($\langle S_z \rangle$) [21, 47]. In this case, when s states in the conduction band are occupied

Table 1. Properties of the magnetic transition metals, showing the moments (m) in Bohr magnetons, after Guimarães [14], the exchange integrals (J) in eV after Brooks [6], the exchange splittings (ΔE_{ex}), obtained from first-principles local spin-density calculations for Fe, Co and Ni by Huang [16] and $Ni_{80}Fe_{20}$ by Davis [11], the molar volumes (v) after Lof [26], and the constant α which is the product of J and v. The moment and exchange splitting for $Ni_{80}Fe_{20}$ have been obtained from first-principles calculations by the authors, and the exchange integral for $Ni_{80}Fe_{20}$ is an interpolation between those of Fe and Ni.

Element	m	J	ΔE_{ex}, mJ	ΔE_{ex} (calculated)	Molar volume (v)	Jv, α
Fe	2.216	0.900	1.98	1.99	7.137	6.42
Co	1.715	0.940	1.61	1.77	6.712	6.31
$Ni_{80}Fe_{20}$	1.01	0.961	0.97	1.14	6.580	6.42
Ni	0.616	0.975	0.60	0.621	6.631	6.47

by electrons, the conduction band is split by exchange interactions between the conduction electron spins and the fluctuating local moments arising from the localized ferromagnetically ordered f states. The exchange splitting of the itinerant states is proportional to $\langle S_z \rangle$ for the f moments. This is similar to the double-exchange model [17, 51] that links the exchange splitting of itinerant states to $M(T)$ through the thermally averaged local moments. An analogous treatment of the 3d ferromagnets would have itinerant electrons occupying a highly dispersive band that is split by an exchange interaction with a band containing more localized ferromagnetically ordered d-electron states [17]. This is reasonable, since the itinerant states are by definition delocalized in space, and can interact with a number of local moments within a certain neighbouring volume, or average moment per volume, $M(T)$. Therefore, regardless of whether the average moment is suppressed with increasing temperature due to a shift of spectral weight (Stoner excitations), or due to magnon-induced precession (spin waves), or due to spin fluctuations, we expect ΔE_{ex} for the itinerant states to be proportional to $M(T)$.

3. Identifying the states that tunnel (the effective tunnelling band structure)

Stearns [44] proposed that only a portion of the band structure comprising d electrons of T_{2g} symmetry are mobile enough to contribute significantly to the tunnelling conductance and thus the spin polarization of the tunnelling electrons. These *itinerant* T_{2g} electrons are nearly as mobile as s electrons and account for the observed polarization of the tunnelling current from 3d ferromagnets. First-principles calculations by Butler *et al* for a [100] Fe/ZnSe/Fe [8] MTJ and a [100] Fe/MgO/Fe [7] MTJ confirmed Stearn's hypothesis. In their work, they showed that bands with Δ_1 symmetry coupled to similar-symmetry evanescent states in the gap of the barrier, and as a result decayed more slowly in the barrier. The decay rate was shown to be determined by the imaginary part of the wavevector of the state. In the case of a simple step barrier where the states inside the gap are simple decaying exponentials, the different decay rates observed for different symmetry states in the leads can be understood from a Fourier analysis of the lead state, since if the appropriate state has a periodic structure in the plane of the interface with a finite smallest reciprocal-lattice vector g_{min}, then the decay in the barrier is determined by $\kappa = \sqrt{(2m^*/\hbar^2)(V_{bar} - E) + (k_{\|} + g_{min})^2}$.

As an example, we show the calculated bands in hcp cobalt in figure (1), along with the fitted parabolas for the tunnelling bands used in the tunnelling calculations, superimposed.

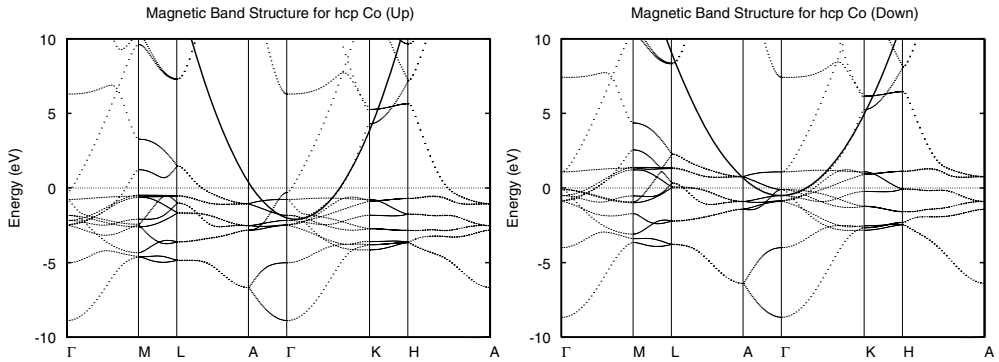

Figure 1. The exchange-split band structure of hcp cobalt calculated from first principles [16]. Parabolas have been superimposed to emphasize the free-electron nature of the bands along the Γ–K direction.

4. Calculation of the conductance

The conductance (G) is obtained from the Landauer–Büttiker formulation [3, 22], where

$$G = \frac{e^2}{(2\pi)^2 h} \int_{E_F - V_{\rm bias}}^{E_F} \mathrm{d}E \int \mathrm{d}^2 k_\parallel \, T(E, k_\parallel). \tag{5}$$

The transmission coefficient is obtained by matching the wavefunction and particle flux at each interface. The barrier states are, of course, given in this model by Airy functions, though we have found by direct computation that the WKB approximate solutions are adequate for the range of bias voltages studied in this article. The general expression for finite-bias tunnelling through the barrier, in the asymptotic limit of zero applied bias voltage and a thick barrier where the transmission coefficient is dominated by states at the Brillouin zone centre and where the effective masses of the electrons in each region are all the same, has a transmission coefficient that takes the particularly simple form

$$T = \frac{4k_1\kappa^2 k_3 \mathrm{e}^{-2d\kappa}}{(V_b - V_1)(V_b - V_3)}. \tag{6}$$

In the above, $V_b - V_1$ ($V_b - V_3$) is the barrier height above the energy zero of the left-hand (right-hand) electrode, d is the barrier thickness, and κ describes the decay of the wavefunction within the barrier. This asymptotic expression explicitly shows the influence of barrier height and thickness, as well as that of the exchange splitting between the bands. We also see that the transmission probability depends on the DOS since k_1 and k_3 are proportional to the DOS for free electrons. The transmission coefficient (T-matrix) for a finite-thickness barrier with different electronic effective masses in each region, or an asymmetric barrier potential, or a barrier with a finite applied bias voltage, is more complicated. Nonetheless, the dependence on exchange splitting and barrier geometry have similar effects.

In our model, the chemical potential of the downstream electrode is shifted down by the applied bias. Since the transmission coefficient is small, this ensures that both leads remain approximately charge neutral. There are now a range of occupied states in a window of energy from the Fermi energy minus the bias voltage to the Fermi energy, and a range of unoccupied states from the Fermi level to the Fermi level plus the bias voltage in the other electrode which participate in the transport.

Now we consider the effects of temperature. The Fermi–Dirac distribution will have an effect on the conductance because the occupancy of the electronic states near the Fermi energy

will vary with temperature. We also include temperature dependence of the magnetization in the electrodes since we have argued that it determines the exchange splitting of the itinerant states. Therefore, in order to include the effect of temperature on the magnetic band structure, we simply allow the zero-temperature splitting and the difference between the effective masses for the two spin channels to collapse at the same rate as $M(T)$ in the electrodes [12, 13, 20], since at the critical temperature, all the tunnelling electrons are assumed to share a common paramagnetic band.

As a result, the polarization, P, now also depends on temperature. We emphasize that at finite applied bias and temperature, electronic states from above and below the Fermi level (where P is different) participate in the tunnelling. If the average polarization of all the participating states is less than that at the Fermi level, then the TMR will be smaller. P is not in general linear in M, but for the types of tunnelling bands that we fitted, we find numerically an approximately linear relation [10] as seen experimentally [30, 31, 48, 49]. Our calculations suggest that knowledge of the bands which supply the tunnelling states and the magnetization curves which describe $M(T)$ at the interfaces is sufficient for predicting the temperature behaviour of the TMR.

5. Using the model

For specific MTJs, we used published $M(T)$ curves [4] to predict the temperature variation of the effective masses and exchange splitting of the tunnelling bands. Intrinsic to these curves are all the excitations which cause M to vary with T. We have noted that $M(T)$ at the interfaces will probably differ from the bulk $M(T)$, but that the shape of the curve will be qualitatively similar in that it is still essentially Bloch-like in the temperature range of interest. The differences between bulk and surface $M(T)$ are in the Bloch coefficients and exponents (B and β) in equation (7):

$$M_s(T) = M_s(0)(1 - BT^{\beta}). \tag{7}$$

A surface $M(T)$ often has Bloch coefficients 2–3 times the bulk value [33]. The surface magnetization curve of a $Fe_xNi_yB_z$ ferromagnetic metallic glass investigated by Pierce *et al* [38] is fitted with a Bloch coefficient that is about 2.8 times that of the bulk value. Additionally, lower-dimension systems are expected to exhibit a suppressed T_c [2]. Strong experimental evidence that it is the interface electronic and magnetic properties that determine the TMR is provided by LeClair *et al* [25]. In this work the Cu was deposited at the interface between the ferromagnetic lead and the barrier and a rapid exponential quenching of the TMR was measured as a function of the Cu layer thickness.

We define the band structure by extracting the Fermi energy, effective masses, and energy minima of the split parabolic tunnelling bands from calculated band structures such as that of figure 1. The effective masses are found by fitting a parabola to the calculated bands for each spin channel. The parameters for bulk hcp Co are $\Delta E_{ex} = (V_{\downarrow} - V_{\uparrow}) = 1.67$ eV, $m^*_{\uparrow} = 1.77$, $m^*_{\downarrow} = 1.58$ with E_F positioned about 2.2 eV above the bottom of the spin-up band. We would like to reiterate that there will be some difference between bulk parameters and those which might be found in the interface regions, and that allowing ΔE_{ex}, m^* and the position of the bottom of the tunnelling band with respect to the Fermi energy to vary in a narrow range may give better fits to experimental data.

The barrier is represented at zero bias by a step potential (or trapezoid for asymmetric barriers), and when the junction is biased the applied voltage is assumed to be dropped uniformly in the barrier region. Typically, Simmons' [41] theory in conjunction with I–V curves can be used to estimate effective parameters for the barrier (d and V_{bar}). A consequence

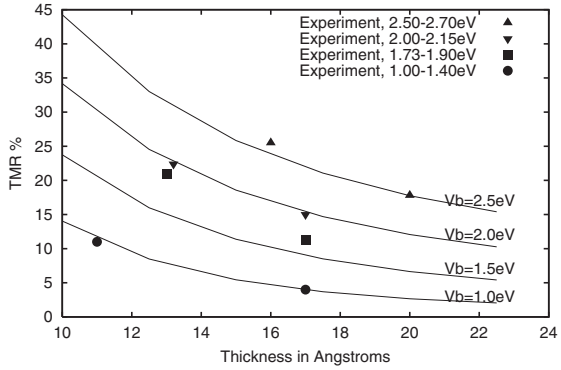

Figure 2. The thickness dependence of the TMR, comparing various experiments [33, 34, 37, 39, 43, 45, 46, 52], and compared to a calculations for a generic Co/I/Co MTJ.

of this is that by relying on the shape of the I–V curves, one obtains different parameters for the parallel and antiparallel configurations. This is due to the fact that the Simmons model does not specifically treat the spin-polarized electronic structure in the leads, but rather lumps the effects of the band structure into an effective barrier. Therefore, we tend to use the actual physical thickness of the barrier if it is known and make the effective barrier height an adjustable parameter whose value is close to the average value obtained by a Simmons fit. The model also allows for the effective mass in the barrier to be specified. We have assumed in the work presented here that $m^* = 1$ in the barrier.

6. Results

In this section, we will present the results of some tunnelling calculations. In figure 2, we have plotted experimental data for zero bias for the TMR, grouped such that points with similar barrier height but different thickness share the same symbol. Curves showing the calculated thickness dependence for various barrier heights have been plotted with the experimental data. In the figure we see good agreement with the measured TMR values and trends as regards the thickness and the barrier height. As can be seen, higher thinner barriers produce a higher TMR. Strikingly, most of the experiments fall near the calculated results despite the fact that the composition of the junction electrodes spans a range of compositions from Fe to Co to Ni and their alloys. The common thread is that all of the electrodes have similar polarizations suggesting that the effective tunnelling band structures of the various electrode compositions are similar.

The origin of the trend of decreasing TMR with barrier thickness reflects the increasing dominance of states at the zone centre on the conductance as the barrier thickness is increased. Thinner barriers on the other hand include contributions to the conductance from states away from the zone centre and thus the different sizes of the Fermi spheres for the two spin-polarized tunnelling bands are important.

Figure 3 shows the calculated effect of barrier height on the TMR at zero bias. We observe a monotonic increase in the TMR with increasing barrier height and decreasing barrier thickness. The dependence on barrier height does not appear to have a simple intuitive explanation, but rather follows from the dependence of the T-matrix on the barrier height. Unlike the case for thickness, the barrier height dependence is not confined to the exponential term in the T-matrix but plays a prominent role in the prefactor as well. While increasing the barrier height tends

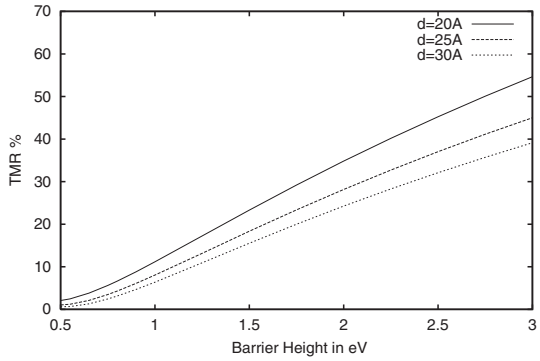

Figure 3. The dependence of the TMR on the barrier height for a tunnel junction with Fe leads using effective masses of $1.3m_e$.

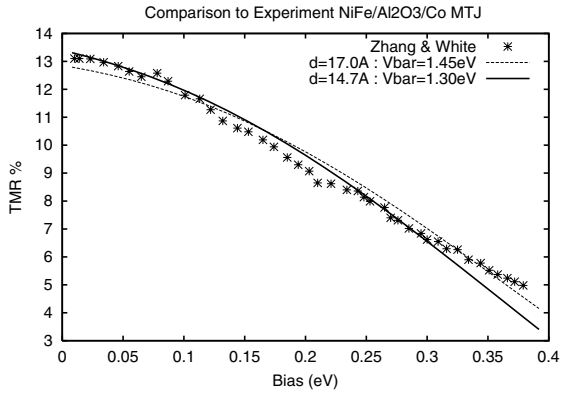

Figure 4. The bias dependence of an Fe|Al_2O_3|Fe junction compared to data published by Zhang and White [52].

to lower the TMR for exactly the same reasons as explain the decrease with increasing barrier thickness, the prefactor, which reflects the wavefunction-matching conditions, dominates and causes the TMR to increase with increasing barrier height.

Next we consider how barrier parameters influence the bias dependence of the TMR. As an example of the level of accuracy obtained from the model, we have calculated the dependence of the TMR on applied bias for an Fe|Al_2O_3|Fe junction and compared it to data published by Zhang and White [52]. The results of the calculation are shown in figure 4. As can be seen, both the magnitude of the TMR and the shape of the bias dependence of the TMR are fitted quite well by parametrized barriers whose thickness and height are close to the reported values. A unique barrier fit can be obtained if the I–V curves are also known, and we have performed this type of analysis for several Co|Al_2O_3|Co tunnel junctions [9–11].

The model can be used to predict effect of applied bias on junctions with different barrier parameters. Control over barrier height can be achieved to some extent by the method of oxidation chosen to form the barrier. For illustration, we have plotted the normalized TMR in figure 5 for a Co_{hcp}|Al_2O_3|Co_{hcp} tunnel junction. The lower the barrier height, the more severe the bias dependence. This behaviour can be understood by realizing that at finite bias we have an effective barrier. The smaller the true barrier height at zero bias in relation to the bias voltage, the greater the effect of bias and the greater the percentage reduction in the TMR. This conclusion is consistent with previous studies [34].

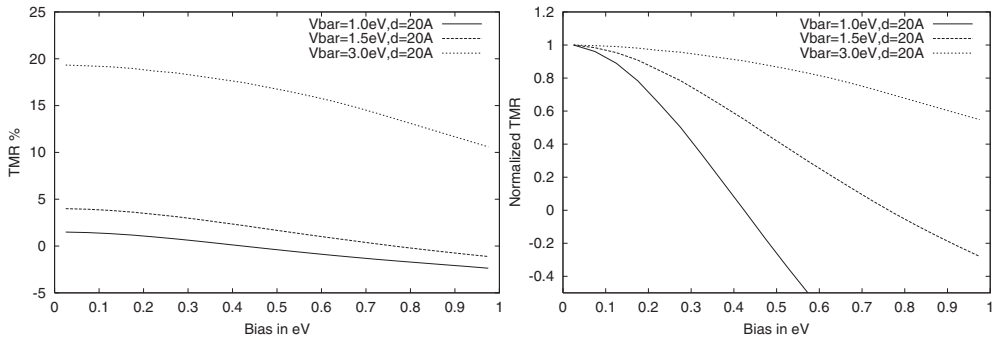

Figure 5. The barrier height dependence of TMR($V_{\rm bias}$) for an hcp-Co-based junction. A larger more robust TMR($V_{\rm bias}$) is predicted for higher barriers.

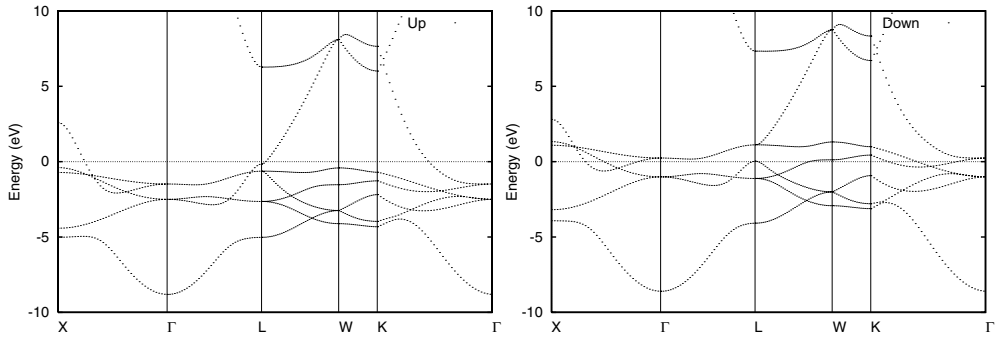

Figure 6. The magnetic band structure of fcc Co. Note the highly dispersive minority band in the Γ–K direction that begins above the Fermi level.

We note often experimentally that, as Co has a small stacking fault energy, the Co electrodes may exhibit mixed fcc and hcp phases. We find that calculations using the hcp Co bands consistently give a lower TMR than those using a combination of fcc and hcp Co bands. This has been observed experimentally by LeClair *et al* [24] and can be understood by noting in figure 6 that the minority tunnelling band along the Γ–K direction in fcc Co is unoccupied (begins above E_F), so the contribution to the tunnelling conductance is very highly polarized, leading to the prediction of a higher TMR for fcc–hcp mixed systems as the relative amount of the fcc phase increases.

Figure 7 shows the variation in the TMR with applied voltage for several barrier thicknesses. On a percentage basis, thinner barriers with a higher initial TMR ratios show the mildest reduction with applied bias, as expected [33, 46]. The decrease in the TMR with increasing thickness results from an approach to the asymptotic limit derived by Slonczewski [42]. In this limit, the current arises only from states with parallel crystal momentum ($k_\parallel$) equal to zero, since states with any parallel momentum will decay too severely to contribute to the tunnelling conductance. Thus differences in current resulting from differences in the majority- and minority-Fermi-sphere sizes are eliminated. The polarization of the tunnelling current and hence the TMR goes down because the reduction in participating majority states is more serious than for the minority states. This appears to be a universal effect since it depends on the barrier parameters.

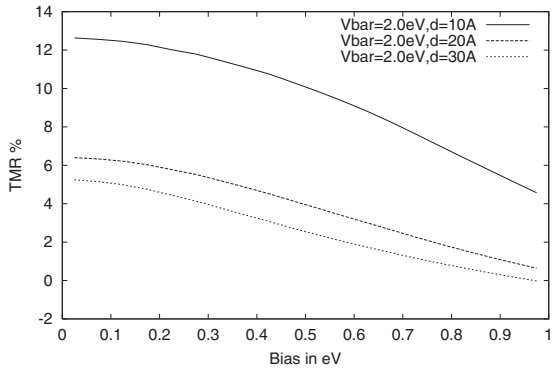

Figure 7. Thickness dependence of the TMR as a function of bias for an hcp-Co-based tunnel junction. A higher TMR is predicted for thinner barriers.

It is worth pointing out that while the model predicts that thinner barriers produce higher values of the TMR, experimentally very thin barriers show a quenching of the TMR which is thought to result from magnetic coupling between electrodes (orange-peel coupling), or because very thin high-quality barriers are difficult to form. As a result, the tunnelling conductance may be augmented by current that is less polarized via pinholes or because coupling between electrodes prevents complete attainment of the antiparallel state. The practical effect of further reduction of the barrier thickness below a certain critical thickness is a suppression (masking) of the intrinsic thickness dependence [36].

It is also interesting to note that increasing V_{bar} has the opposite effect on the TMR to increasing d. This means that there are a range of thickness–height pairs which can produce the correct TMR. However, since increasing either parameter suppresses conductance, only one V_{bar}–d pair can simultaneously produce the correct TMR and current density. Furthermore, insight into the effective tunnelling bands can also be gained if one allows the description of the bands to vary slightly until the correct $\Delta\mathrm{TMR}(V_{\mathrm{bias}})$ is also produced. We have tested the model against data for several MTJs and found that it is possible to simultaneously match current density and $\mathrm{TMR}(V_{\mathrm{bias}})$ with parameters for the barrier very close to the deduced starting parameters.

Next we wish to study the temperature dependence. Our model is based on the observation that the tunnelling bands appear to behave as in a Stoner picture, and that at low temperatures (relative to the Curie temperature) the exchange splitting is proportional to the magnetization. In figure 8 we compare the calculated TMR versus temperature against experimental values obtained from the literature for two different tunnel junctions. Using bulk magnetization curves produces a fall off in the TMR that is less rapid than that in experiment. However, by increasing the parameter B, or alternatively reducing the Curie temperature, the magnetization can be made to fall off more rapidly. The fitted curves have a fall off in the magnetizations at low temperatures of about twice the bulk value, which is not inconsistent with measured surface and interface magnetic behaviour.

As in the case of our studies on the influence of bias voltage on the TMR, figure 9 shows that $\Delta\mathrm{TMR}(T)$ is sensitive to the barrier geometry and that high thin barriers produce the highest TMR. We can also see that on a percentage basis, high thin barriers produce the mildest $\Delta\mathrm{TMR}(T)$ for temperatures below 300 K, but at intermediate temperatures $\Delta\mathrm{TMR}(T)$ increases dramatically for these barriers. This means that for small changes in M such as occur between zero and room temperature, large changes in the TMR can occur, and that near T_{C} where M is experiencing its greatest decay, the rate of change of the TMR might be quite mild.

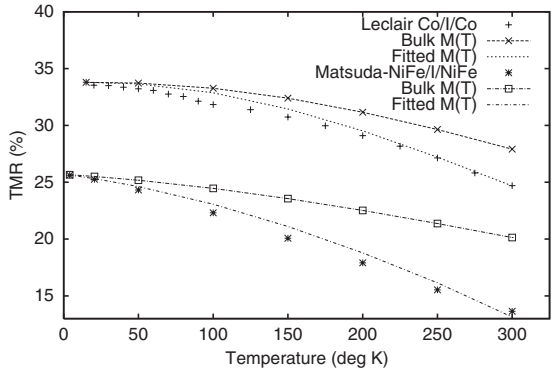

Figure 8. The temperature dependence of the TMR obtained using the bulk magnetization versus temperature curves and magnetization curves that reduce the value of M at a rate that is a function of bias for an hcp-Co-based tunnel junction. A higher TMR is predicted for thinner barriers.

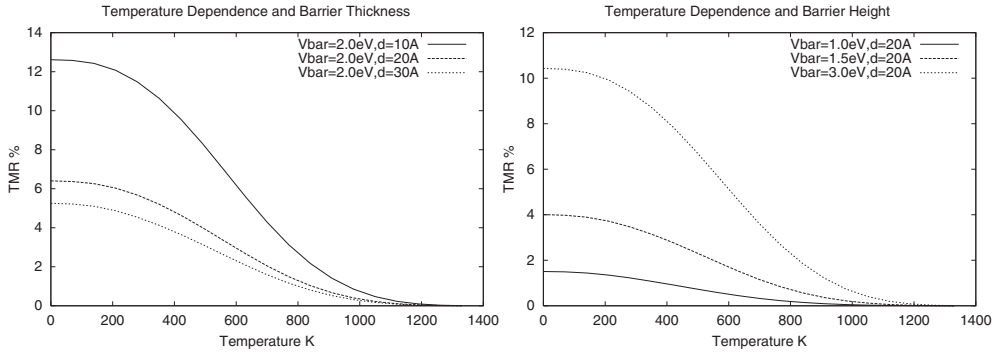

Figure 9. The barrier geometry and TMR(T) for a hcp-Co-based tunnel junction. High thin barriers yield a higher TMR.

This explains quite well the observation that the TMR seems to fall much more quickly with temperature than does either P or M [17, 35].

The final issue that we would like to discuss concerns the asymmetry in the TMR of a tunnel junction under forward and reverse applied bias voltages. There are several ways in which such an asymmetry can arise. One way is if the electronic structures of the tunnelling states in the two leads differ; another is if the interfaces themselves differ; while another is if the barrier itself has asymmetry. Asymmetry could be expected in many MTJs since there are clear differences in growth for the two electrodes. The first electrode is deposited on a carefully prepared buffer while the other is deposited on a rough amorphous Al_2O_3 surface. This explains the observation that otherwise-identical electrodes might produce an asymmetric response. In fact LeClair *et al* [24] have grown Co|Al_2O_3|Co MTJs where both Co electrodes have been grown as a mixture of hcp and fcc phases and others where the fcc phase dominates the mix in one of the electrodes. In this work, they only find significant asymmetry in the latter group of MTJs. This strongly suggests that when the two electrodes have different electronic structures, an asymmetric TMR results. This case provides one of the most dramatic examples of an asymmetric response, and this can be traced back to the underlying band structure. In figure 6, we can see for fcc Co that the minority tunnelling band is unoccupied. Hence in one direction of the applied bias, which lowers the chemical potential of the fcc Co with respect

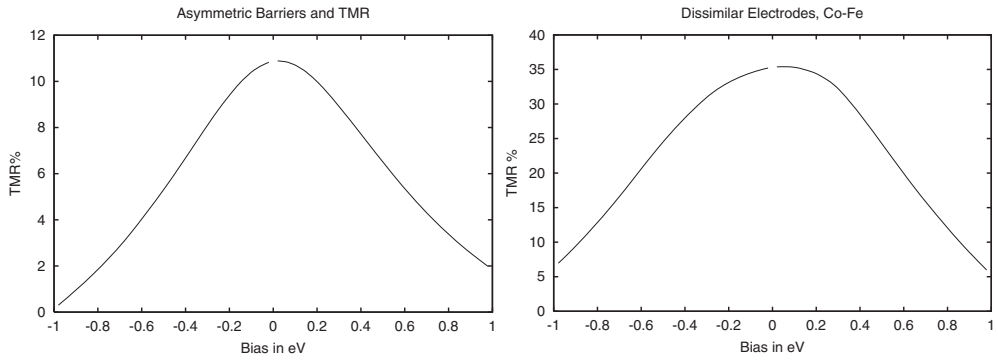

Figure 10. The asymmetry in a theoretical Co|Al_2O_3|Fe MTJ (dissimilar electrodes), and the asymmetry due to an asymmetric barrier in a Co|Al_2O_3|Co MTJ. The difference in barrier height between the two interfaces was 0.5 eV.

to the hcp Co electrode, this 'unoccupied' band can accept electrons and contribute to the conductance. However, biasing in the opposite sense keeps this band unoccupied and so it does not contribute to the conductance.

Brückl *et al* [5] showed that Cu migrating into the interface region of a Co|Cu|Co|Al_2O_3|Co MTJ during annealing produces a large asymmetry in the I–V (and TMR) characteristics. This produced a Cu–Al_2O_3 intermixing zone that modified the barrier at that interface, which strongly suggests that an asymmetric barrier can produce an asymmetric response. Calculations with asymmetric barriers reflecting intermixing at one interface only do indeed reproduce the asymmetry [11].

As an example we have computed the expected TMR for asymmetric junctions, one with different electrodes, the other with an asymmetric barrier chosen to represent the type of alloyed barrier studied by Brückl. As can be seen in figure 10 the TMR for positive applied bias differs from that for negative applied bias. In the case of a junction fabricated from different ferromagnets, this type of asymmetric response may be of benefit. Since all devices are operated at finite bias, such junctions may take advantage of the slower fall-off in TMR for one bias direction, while utilizing the properties of the different magnetic layers to control switching and allowing one layer to be pinned with the other free to rotate in the presence of an applied magnetic field.

7. Conclusions

We have presented a straightforward treatment of spin-dependent tunnelling in a MTJ with inputs for the tunnelling states in the two ferromagnetic leads provided by first-principles calculations and a simple step-potential model of the barrier region whose height is consistent with the band gap of the barrier. This model can quantitatively reproduce the observed zero-bias TMR in many experimental samples. At finite applied voltage, we assume that the potential is dropped only in the insulating barrier region and that this can be modelled by a simple linear potential. Such a model also reproduces the observed bias dependence and the asymmetry when the two electrodes differ. This model allowed us to explore the role of various parameters in the TMR leading us to the conclusion that thin high barriers offer the greatest response for a given set of ferromagnetic electrodes. The benefits of a thin barrier were that states away from the zone centre contributed to the current, and thus the differently sized Fermi spheres of majority and minority carriers impacted on the conductance. The currents in thick barriers were dominated only by states near the zone centre. The role of biasing could be interpreted in terms of an effective barrier and the decrease in polarization of the states at higher energies.

We have also applied our model to a study of the influence of temperature, including Fermi–Dirac statistics and a Stoner model of the exchange splitting of the itinerant tunnelling states. This model was suggested by photoemission studies that showed for the 3d ferromagnets that the exchange splitting of these states collapsed at the Curie temperature; published magnetization data can produce nearly all of the observed characteristics of the experimental response. We conclude that the temperature dependence arises primarily because the exchange splitting of the itinerant portion of the band structure collapses as the temperature increases. Even though the change in magnetism is small at lower temperatures, a large change in the TMR can be seen—though in order to reproduce experimental decreases in the TMR, we need to make the magnetization fall off more rapidly. A more rapid decrease with temperature is not unexpected for an interface or surface. The extreme sensitivity of tunnelling to the interface electronic structure was confirmed in experiments by LeClair *et al* where a single monolayer on non-magnetic Cu was sufficient to quench the TMR.

Finally the model shows that asymmetry can arise from an asymmetric barrier or from differences between the descriptions of same-spin states on either side of the barrier. The main effect of asymmetry is to shift the maximum of the TMR away from zero bias, opening up the possibility that MTJs could be engineered with a specified optimum operating voltage [11].

Acknowledgments

Many thanks to Patrick LeClair and Hubert Brückl for data and comments concerning the TMR in cobalt-based MTJs. Support at Tulane University was provided by DARPA grant MDA 972-97-1-003, and NSF-EPSCoR award NSF/LEQSF (2001-04-RII-03).

References

[1] Aebi P, Kreutz T J, Osterwalder J, Fasel R, Schwaller P and Schlapbach L 1996 *Phys. Rev. Lett.* **76** 1150
[2] Bander M and Mills D L 1988 *Phys. Rev.* B **38** 12 015
[3] Büttiker M 1988 *IBM J. Res. Dev.* **32** 317
[4] Bozorth R M 1993 *Ferromagnetism* (New York: IEEE)
[5] Brückl H, Schmalhorst J, Reiss G, Gieres G and Wecker J 2001 *Appl. Phys. Lett.* **78** 1113
[6] Brooks M S S 1997 Conduction electrons in magnetic metals *Symp. in Memory of Allan Mackintosh* ed J Tensen, D F McMorrow and H M Rønnow (Copenhagen: Royal Danish Academy of Science and Letters)
[7] Butler W H, Zhang X G, Schulthess T C and MacLaren J M 2001 *Phys. Rev.* B **63** 54 416
[8] Butler W H, Zhang X G, Schulthess T C, Nicholson D M C, Oparin A B and MacLaren J M 1999 *J. Appl. Phys.* **85** 5834
[9] Davis A H and MacLaren J M 2000 *J. Appl. Phys.* **87** 5224
[10] Davis A H, MacLaren J M and LeClair P 2001 *J. Appl. Phys.* **89** 7567
[11] Davis A H 2000 Spin dependent tunneling in magnetic tunnel junctions *PhD Thesis* Tulane University, New Orleans, LA (available upon request)
[12] Donath M, Gubanka B and Passek F 1996 *Phys. Rev. Lett.* **77** 5138
[13] Greber T, Kreutz T J and Osterwalder J 1997 *Phys. Rev. Lett.* **79** 4465
[14] Guimarães A P 1998 *Magnetism and Magnetic Resonance in Solids* (New York: Wiley)
[15] Heide C and Elliott R J 2000 *Europhys. Lett.* **50** 271
[16] Huang Weidong 1999 Theoretical studies of the magneto-optical effects in metals *PhD Thesis* Tulane University, New Orleans, LA
[17] Itoh H, Ohsawa T and Inoue J 2000 *Phys. Rev. Lett.* **84** 2501
[18] Julliere M 1975 *Phys. Lett.* **54** 225
[19] Kisker E, Schroder K, Campagna M and Gudat W 1984 *Phys. Rev. Lett.* **52** 2285
[20] Kreutz T J, Greber T, Aebi P and Osterwalder J 1998 *Phys. Rev.* B **58** 1300
[21] Kubo K 1974 *J. Phys. Soc. Japan* **36** 32
[22] Landauer R 1957 *IBM J. Res. Dev.* **1** 223

[23] LeClair P, Kohlhepp J T, van de Vin C H, Wieldraaijer H, Swagten H J M, de Jonge W J M, Davis A H, MacLaren J M, Jansen R and Moodera J S 2001 Observation of band structure and density of states effects in Co-based magnetic tunnel junctions *Phys. Rev. Lett.* submitted
[24] LeClair P, Kohlhepp J T, van de Vin C H, Wieldraaijer H, Swagten H J M, de Jonge W J M, Davis A H, MacLaren J M, Moodera J S and Jansen R 2002 *Phys. Rev. Lett.* **88** 107201
[25] LeClair P, Swagten H J M, Kohlhepp J T, van de Veerdonk R J M and de Jonge W J M 2000 *Phys. Rev. Lett.* **84** 2933
[26] Lof P 1987 *Elsevier's Periodic Table of the Elements* (Amsterdam: Elsevier Science)
[27] MacDonald A H, Jungwirth T and Kasner M 1998 *Phys. Rev. Lett.* **81** 705
[28] MacLaren J M, Zhang X G and Butler W H 1997 *Phys. Rev.* B **56** 11 827
[29] Mathon J 1997 *Phys. Rev.* B **56** 11 810
[30] Mauri D, Scholl D, Siegmann H C and Kay E 1988 *Phys. Rev. Lett.* **61** 758
[31] Meservey R, Paraskevopoulos D and Tedrow P M 1976 *Phys. Rev. Lett.* **37** 858
[32] Mitsuzuka T, Matsuda K, Kamijo A and Tsuge H 1999 *J. Appl. Phys.* **85** 5807
[33] Moodera J S, Nowak J and van de Veerdonk R J M 1998 *Phys. Rev. Lett.* **80** 2941
[34] Moodera J S and Kinder L R 1996 *J. Appl. Phys.* **79** 4724
[35] Moodera J S, Kinder L R, Wong T M and Meservey R 1995 *Phys. Rev. Lett.* **74** 3273
[36] Moodera J S and Mathon G 1999 *J. Magn. Magn. Mater.* **200** 248
[37] Oepts W, Verhagen H J, Coehoorn R and de Jonge W J M 1999 *J. Appl. Phys.* **86** 3863
[38] Pierce D T, Celotta R J, Unguris J and Siegmann H C 1982 *Phys. Rev.* B **26** 2566
[39] Shang C H, Jansen R, Nowak J and Moodera J S 1998 *Phys. Rev.* B **58** 2917
[40] Shimizu M, Katsuki A, Yamada H and Terao K 1966 *J. Phys. Soc. Japan* **21** 1654
[41] Simmons J G 1963 *J. Appl. Phys.* **34** 1793
[42] Slonczewski J C 1989 *Phys. Rev.* B **39** 6995
[43] Sousa R C, Sun J J, Soares V, Freitas P P, Kling A, Da Silva M F and Soares J C 1999 *J. Appl. Phys.* **85** 5258
[44] Stearns M B 1977 *J. Magn. Magn. Mater.* **5** 167
[45] Sun J J and Freitas P P 1999 *J. Appl. Phys.* **85** 5264
[46] Sun J J, Sousa R C, Galvão T T P, Soares V and Freitas P P 1999 *J. Magn. Soc. Japan* **23** 55
[47] Takahashi M and Mitsui K 1996 *Phys. Rev.* B **54** 11 298
[48] Tedrow P and Meservey R 1971 *Phys. Rev. Lett.* **26** 191
[49] Tedrow P M and Meservey R 1973 *Phys. Rev.* B **26** 318
[50] Uiberacker C, Wang K, Heide C and Levy P M 2001 *J. Appl. Phys.* **89** 7561
[51] Zener C 1951 *Phys. Rev.* **82** 403
[52] Zhang J and White R M 1998 *J. Appl. Phys.* **83** 6512
[53] Zhang S, Levy P M, Marley A C and Parkin S S S 1997 *Phys. Rev. Lett.* **79** 3744
[54] Zhang X, Li Bo-Zang, Sun G and Pu F 1997 *Phys. Rev.* B **56** 5484